HHS Public Access

Author manuscript

*Cell Metab*. Author manuscript; available in PMC 2016 March 03.

Published in final edited form as:

*Cell Metab*. 2015 March 3; 21(3): 493–501. doi:10.1016/j.cmet.2015.02.003.

# Cutaneous $Na^+$ storage strengthens the antimicrobial barrier function of the skin and boosts macrophage-driven host defense

**Jonathan Jantsch**[1,2,14], **Valentin Schatz**[1,2,14], **Diana Friedrich**[1,3,14], **Agnes Schröder**[3], **Christoph Kopp**[3], **Isabel Siegert**[1], **Andreas Maronna**[4], **David Wendelborn**[1,3], **Peter Linz**[3], **Katrina J. Binger**[9,10], **Matthias Gebhardt**[9,10], **Matthias Heinig**[10,11], **Patrick Neubert**[3], **Fabian Fischer**[1], **Stefan Teufel**[6,7], **Jean-Pierre David**[6,7], **Clemens Neufert**[8], **Alexander Cavallaro**[5], **Natalia Rakova**[9], **Christoph Küper**[12], **Franz-Xaver Beck**[12], **Wolfgang Neuhofer**[12], **Dominik N. Muller**[9,10], **Gerold Schuler**[4], **Michael Uder**[5], **Christian Bogdan**[1], **Friedrich C. Luft**[9,13], and **Jens Titze**[3,13]

[1]Microbiology Institute – Clinical Microbiology, Immunology and Hygiene, Universitätsklinikum Erlangen and Friedrich-Alexander Universität (FAU) Erlangen-Nürnberg, Erlangen, Germany

[2]Institute of Clinical Microbiology and Hygiene, Universitätsklinikum Regensburg and Universität Regensburg, Regensburg, Germany

[3]Interdisciplinary Center for Clinical Research and Department of Nephrology and Hypertension, Universitätsklinikum Erlangen and Friedrich-Alexander Universität (FAU) Erlangen-Nürnberg, Germany

[4]Department of Dermatology, Universitätsklinikum Erlangen and Friedrich-Alexander Universität (FAU) Erlangen-Nürnberg, Germany

[5]Department of Radiology, Universitätsklinikum Erlangen and Friedrich-Alexander Universität (FAU) Erlangen-Nürnberg, Germany

[6]Department of Internal Medicine 3, Rheumatology and Immunology, Universitätsklinikum Erlangen and Friedrich-Alexander Universität (FAU) Erlangen-Nürnberg, Germany

[7]Institute for Osteology and Biomechanics, University Medical Center Hamburg-Eppendorf, Hamburg, Germany



Contact information: Jonathan Jantsch, MD, Institute of Clinical Microbiology and Hygiene, Universitätsklinikum Regensburg and Universität Regensburg, Franz-Josef-Strauß-Allee 11, 93053 Regensburg, Germany. Tel. +49-941-944 6401, FAX +49-941-944 6402, Jonathan.Jantsch@ukr.de.

[14]Co-first author

**Author Contributions**

V.S., D.F., A.S., J.J., I.S., F.F., P.N., P.L., C.Ko., D.W., S.T., K.J.B., M.G., M.H., N.R., C.Kü., D.N.M. and J.T. did experiments and analyzed the data. A.M., A.C., P.L. C.Ko., M.U. and G.S. enrolled patients and performed MRI. C.B., C.Kü., S.T., J.P.D., C.N., F.X.B, D.N.M., K.J.B. and W.N. provided essential material and contributed to the design of the experiments. D.N.M., D.F., K.J.B., P.L. and V.S. contributed to manuscript preparation. K.J.B., D.N.M., J.J. and J.T. designed and planned the experiments, analyzed and interpreted data. J.J., C.B., F.C.L, and J.T. wrote the manuscript.

[8]Department of Internal Medicine 1, Universitätsklinikum Erlangen, Friedrich-Alexander-Universität Erlangen-Nürnberg

[9]Experimental and Clinical Research Center (ECRC), Experimental and Clinical Research Center, an institutional cooperation between the Charité Medical Faculty and the Max-Delbrück Center for Molecular Medicine, Berlin, Germany

[10]Max-Delbrück Center for Molecular Medicine, Berlin Germany

[11]Department of Computational Biology, Max Planck Institute for Molecular Genetics, Berlin, Germany

[12]Department of Physiology, Ludwigs-Maximillians Universität München, Munich, Germany

[13]Divison of Clinical Pharmacology, Vanderbilt University School of Medicine, Nashville, Tennessee, USA

## Summary

Immune cells regulate a hypertonic microenvironment in the skin; however, the biological advantage of increased skin $Na^+$ concentrations is unknown. We found that $Na^+$ accumulated at the site of bacterial skin infections in humans and in mice. We used the protozoan parasite *Leishmania major* as a model of skin-prone macrophage infection to test the hypothesis that skin-$Na^+$ storage facilitates antimicrobial host defense. Activation of macrophages in the presence of high NaCl concentrations modified epigenetic markers and enhanced p38 mitogen-activated protein kinase (p38/MAPK)-dependent nuclear factor of activated T cells 5 (NFAT5) activation. This high-salt response resulted in elevated type-2 nitric oxide synthase (*Nos2*)-dependent NO production and improved *Leishmania major* control. Finally, we found that increasing $Na^+$ content in the skin by a high-salt diet boosted activation of macrophages in an *Nfat5*-dependent manner and promoted cutaneous antimicrobial defense. We suggest that the hypertonic microenvironment could serve as a barrier to infection.

## Introduction

The skin, the lungs, the intestine and the kidneys are physiological regulators of internal environment composition by forming effective biological barriers which seal our body's constant *milieu intérieur* from an inconstant and hostile external environment. The skin serves as a barrier against physical and chemical assaults, such as dehydration and UV radiation (Proksch et al., 2008). It also forms an antimicrobial barrier that shapes the commensal skin microbiota and prevents invasion of microorganisms (Belkaid and Segre, 2014). The antimicrobial function of this barrier requires the production of antimicrobial peptides and lipids (Braff and Gallo, 2006; Fischer et al., 2014) and the interaction between keratinocytes and immune cells (Schroder, 2010). Experimental modification of skin barrier components culminates in mild to lethal phenotypes (Proksch et al., 2008).

$Na^+$ metabolism may represent an unappreciated functional component of skin barrier formation. Large amounts of $Na^+$ are stored in the skin. Skin $Na^+$ storage can be induced experimentally by dietary salt (Ivanova et al., 1978; Padtberg, 1909; Titze et al., 2004; Wahlgren, 1909). Recent advances in magnetic resonance imaging allow for non-invasive

quantification of $Na^+$ storage in the skin in humans and revealed that cutaneous $Na^+$ stores increase with age (Linz et al., 2015). This age-dependent $Na^+$ accumulation is associated with primary (essential) and secondary hypertension (Kopp et al., 2013; Kopp et al., 2012; Linz et al., 2015). Experimental studies suggest that $Na^+$ storage creates a microenvironment of hyperosmolality in the skin (Wiig et al., 2013), which is also a characteristic feature of inflamed tissue (Paling et al., 2013; Schwartz et al., 2009) and of lymphatic organs (Go et al., 2004).

Immune cells residing in such hypertonic interstitial fluid compartments polarize in response to the osmotic stress and change their function. Mediated by the osmoprotective transcription factor, NFAT5, macrophages (MΦ) exert homeostatic regulatory function in the $Na^+$ overladen interstitium of the skin and regulate $Na^+$ clearance from skin $Na^+$ stores through cutaneous lymph vessels, which lowers systemic blood pressure (Lee et al., 2014; Machnik et al., 2009; Wiig et al., 2013). In contrast, T cells exposed to high salt microenvironments skew into a pro-inflammatory Th17 phenotype, and worsen autoimmune disease (Kleinewietfeld et al., 2013; Wu et al., 2013). High salt diets also aggravated *Helicobacter pylori*-induced inflammation and carcinogenesis (Gaddy et al., 2013).

While current evidence suggests that skin $Na^+$ deposition is linked with disease in humans, the biological advantage of $Na^+$ storage is unknown. We speculate that an underlying biological principle of $Na^+$ metabolism is to generate hypertonic microenvironments as a protective element against outside invaders. Here we show that cutaneous $Na^+$ stores strengthen an immuno-physiological barrier to promote immune-mediated host defense.

## Results

### Infection increases $Na^+$ storage in skin

We visualized skin $Na^+$ content in patients with bacterial skin infection by $^{23}Na$ magnetic resonance imaging ($^{23}Na$ MRI). Infected areas displayed remarkable $Na^+$ accumulation (Fig. 1A–B), which was reduced after antibiotic treatment (Fig. 1A). $^{23}Na$ MRI reliably detects skin-$Na^+$ content, but underestimates $Na^+$-concentrations. Additional $^{23}Na$ spectroscopy revealed enhanced $Na^+$ concentrations in infected human skin (Fig. 1B), which were consistent with $Na^+$-to-water ratios obtained by chemical analysis in bitten mice with infected skin lesions (Fig. 1C). Infected mouse skin displayed ~40 mmol/l increase in ($Na^+$+$K^+$)-to-water ratio, compared to plasma levels (Fig. 1D). These findings suggest that immune cells entering wounded skin are exposed to a hypertonic interstitial microenvironment. We hypothesized that $Na^+$ accumulation within the microenvironment facilitates antimicrobial host defense.

### NaCl boosts MΦ activation

We first tested this hypothesis *in vitro* and investigated the effect of salt on lipopolysaccharide (LPS)-induced classical antimicrobial MΦ activation by analyzing NO and TNF release (Murray and Wynn, 2011). A 40 mM increase in culture medium NaCl concentration (HS) boosted LPS-triggered induction of *Nos2* on mRNA and protein level with enhanced NO release in RAW 264.7 MΦ and bone marrow-derived MΦ (BMM) (Fig.

2A). Parallel experiments with increased concentrations of the tonicity control, urea, (Tab. S1) neither increased *Nos2* expression, nor NO release. Similarly, HS augmented NO release in peritoneal MΦ (Fig. S1A). In line with earlier data (Junger et al., 1994; Shapiro and Dinarello, 1997), HS boosted LPS-induced TNF secretion in MΦ (Fig. S1B–C). HS also triggered NO release in BMM stimulated with IL-1α + TNF or IL-1β + TNF (Fig. 2B). To study epigenetic modifications of the *Nos2* gene, we performed chromatin immunoprecipitation DNA-sequencing (Tab. S2). LPS boosted histone H3 lysine-4 trimethylation (H3K4me3) in the *Nos2* gene (Fig. S1D–E), indicating activation of *Nos2* transcription (Angrisano et al., 2012). HS further augmented H3K4me3 at distinct regions in the *Nos2* gene (Fig. S1D–E). We conclude that HS augments LPS-mediated and IL-1α or IL-1β + TNF-induced MΦ activation.

## Salt-driven MΦ activation depends on p38/MAPK

We next investigated LPS-driven signaling pathways that share HS responses (Denkert et al., 1998; Han et al., 1994; Lang et al., 2002; Shapiro and Dinarello, 1995) and that promote antimicrobial MΦ effector function (Kawai and Akira, 2010; Rauch et al., 2013). LPS-treatment alone uniformly increased JNK (c-JUN N-terminal kinase)/MAPK, p44/42 (extracellular signal-regulated kinases, ERK)/MAPK (Fig. S1F) phosphorylation, activation of nuclear factor ‘kappa-light-chain-enhancer’ of activated B cells (NF-κB; Fig. S1G), and signal transducer and activator of transcription 1 (STAT1; Fig. S1H). HS did not promote the activation of these signaling cascades (Fig. S1F–H). Similarly, *Stat1*-deficiency did not reduce the salt-driven boost in TNF release (Fig. S1I). In contrast, HS augmented LPS-induced phosphorylation of p38/MAPK, its downstream target, MAPK-activated protein kinase 2 (MK2; Fig. 2C), and increased TNF and NO release (Fig. 2D). Pharmacological p38/MAPK blockade abolished MK2 activation (Fig. 2C) and prevented the salt-driven boost in TNF and NO production (Fig. 2D). Similarly, genetic deletion of p38α prevented the salt-driven increase in NO production in LPS-stimulated MΦ (Fig. 2E). The findings suggest that HS boosts proinflammatory MΦ activation via the p38/MAPK signaling cascade.

## p38/MAPK requires NFAT5 for HS-driven boost in MΦ activation

p38/MAPK regulates NFAT5, which is pivotal for HS responses (Ko et al., 2002; Roth et al., 2010). We hypothesized that NaCl enhances p38/MAPK-dependent NFAT5 activation and boosts LPS-induced MΦ function. HS-induced osmotic stress increased NFAT5 protein expression with and without LPS stimulation and p38/MAPK-blockade blunted this response (Fig. 2F). NFAT5 binds to the promoters of osmoprotective genes (Ko et al., 2000; Lopez-Rodriguez et al., 1999; Miyakawa et al., 1999). *Nos2* is a known NFAT5 target gene (Buxade et al., 2012). Whether or not NFAT5 is similarly involved in upregulating *Nos2* and subsequent NO production by HS is unknown. Reducing NFAT5 levels with *Nfat5*-specific small interfering RNA (siRNA) prevented the boost in NO production in LPS-stimulated MΦ exposed to HS-induced osmotic stress (Fig. 2G). In reverse, we found a large increase in NO production in *Nfat5*-overexpressing MΦ with LPS stimulation, even in the absence of a hypertonic microenvironment (Fig. 2H). To demonstrate that NFAT5 was the downstream target of p38/MAPK, we blocked p38/MAPK in control and *Nfat5*-overexpressing MΦ. In contrast to controls, p38/MAPK inhibition did not reduce excess NO production in *Nfat5*-

overexpressing MΦ (Fig. 2I). We conclude that the HS microenvironment boosts MΦ activation via p38/MAPK-dependent NFAT5 signaling. While this specific HS response is independent of STAT1-mediated INF-γ signaling (Fig. 2K), the resulting boost in NO production is as potent as the classical INF-γ-driven activation of NO production in MΦ (Fig. 2G).

## HS promotes leishmanicidal activity via p38/MAPK-dependent NFAT5 signaling

We next tested the effect of HS on MΦ elimination of intracellular *Escherichia (E.) coli* and *Leishmania (L.) major*. Increasing the NaCl concentration in the cell culture medium by 40 mM boosted NO production in *E. coli*-infected MΦ and promoted *E. coli* removal (Fig. 3A). Similarly, HS boosted *L. major* elimination in LPS-treated MΦ (Fig. 3B). This leishmanicidal effect of HS in LPS-stimulated MΦ, which was characterized by increased *Nos2* mRNA expression (Fig. S2A) and NO production, was similar to the effect of IFN-γ co-stimulation ($P_{(\text{HS vs IFN-}\gamma)} = 0.232$). Blocking p38/MAPK-inhibited HS-induced phosphorylation of MK2 (Fig. S2B). This effect was paralleled by less NO production (Fig. S2C) and reduced *L. major* killing in response to HS (Fig. 3C). Similarly, *Nfat5*-deficient MΦ showed reduced NO production (Fig. S2D–E) and a diminished killing efficiency when stimulated with LPS and HS (Fig. 3D). Elimination of *L. major* depends on classical MΦ activation and subsequent NO production (Diefenbach et al., 1998; Liew et al., 1990; Mahnke et al., 2014). Accordingly, the killing of *L. major* was abrogated in LPS-treated *Nos2*$^{-/-}$ MΦ co-stimulated with either HS, or INF-γ (Figures 3E **&** S2F). These findings demonstrate that HS-induced *Leishmania* killing is coordinated by p38/MAPK and NFAT5 activation, which increases *Nos2*-dependent NO production.

## High-salt diet (HSD) ameliorates cutaneous L. major infection in vivo

HSD leads to $Na^+$ accumulation in the skin. We tested the hypothesis that such diet-induced skin $Na^+$ storage may promote the healing of hind footpad infection with *L. major*. Within the first 20 days after infection, footpad thickness increased in mice fed either low-salt diet (LSD) or high-salt diet (HSD; Fig. 4A). LSD mice then showed a non-resolving course of infection with persistent skin lesions, whereas the footpad thickness steadily decreased in HSD mice. Improved healing was paralleled by increased $(Na^+ + K^+)/H_2O$ ratio in HSD mice. This hypertonic microenvironment was accompanied by a significant reduction of *L. major* burden at the end of the experiment ($2^{nd}$ time point; Fig. 4B). We found a tendency towards increased IFN-γ production in HSD mice, suggesting that *Leishmania*-specific T cell responses may be involved in improved host defense with HSD (Fig. 4B). MΦ count was not different between the diet groups (Fig. 4B). In the end of the study, HSD animals showed increased *Nfat5* mRNA levels and elevated NOS2 levels (Fig. 4C). These findings suggest that HSD promotes salt storage in the skin and facilitates leishmanicidal activity by enhancing NOS2-expression, especially during resolution phase of infection. We also studied mice with myeloid cell-specific conditional *Nfat5* gene deletion (Machnik et al., 2009; Wiig et al., 2013) to test the relative contribution of NFAT5 for salt-assisted *L. major* elimination in myeloid cells *in vivo*. LPS-treated BMM from LysM$^{Cre}$*Nfat5*$^{fl/fl}$ mice showed reduced NFAT5 expression and NO production when exposed to salt-induced osmotic stress (Fig. S3). *In vivo*, myeloid cell-specific *Nfat5*-deletion reduced the HSD-driven boost in NOS2 expression in lesional MΦ (Fig. 4D). HSD-control mice had significantly reduced *L.*

*major* load in the skin (Fig. 4D). HSD-LysM$^{Cre}$*Nfat5*$^{fl/fl}$ mice only showed a tendency ($P$ = 0.058) towards *L. major* load reduction and tended to have higher *L. major* burden than controls ($P$ = 0.078). These findings suggest *Nfat5* in myeloid cells/ MΦ improves the boosting of NOS2-expression in MΦ entering the salt-overloaded microenvironment in the skin, and thereby facilitates anti-leishmanial control *in vivo.*

## Discussion

We show in humans and in mice that skin-$Na^+$ accumulation occurs during cutaneous bacterial infections and endogenously boosts antimicrobial capacity in MΦ. Our findings support the idea that salt metabolism is a physiological component in cutaneous immunological barrier formation to ward off infections. Salt deposition might serve as an ancient mechanism to aid in immune-mediated pathogen removal.

### $Na^+$ storage and skin barrier generation

The skin epidermis harbors a liquid-liquid interphase, where tight-junctions compartmentalize the extracellular fluid space and prevent transepidermal water losses (Furuse et al., 2002; Tunggal et al., 2005). Furthermore, active $Na^+$ transport by keratinocytes may create an additional physiological fluid barrier with high osmolality inside or directly under the epidermis (Hofmeister et al., 2015; Warner et al., 1988). High magnetic strength (7 Tesla) $^{23}$Na MRI analyses have confirmed the existence of this $Na^+$-rich fluid layer in the human skin (Linz et al., 2015). Our $^{23}$Na MRI measurements at 3 Tesla underestimate the real skin $Na^+$ concentration, mainly due to partial volume effects arising from a mismatch of MRI resolution (3×3 mm) and thickness of the skin layer (1 mm). To overcome this limitation, we employed $^{23}$Na spectroscopy combined with high-resolution proton imaging. Skin $Na^+$ concentrations obtained with this technology are of the same magnitude order as data obtained by chemical analysis of mouse skin. Our findings suggest that edema formation in infection is not only characterized by water retention and swelling, but also creates a microenvironment of high $Na^+$ concentration. Because direct interstitial fluid collections for osmolality measurements in our patients were not possible in this non-invasive clinical $^{23}$Na MRI study, additional experiments will be necessary to address the relevance of these findings to human disease.

### $Na^+$-enriched skin microenvironment promotes host defense

While the mechanisms by which $Na^+$ is concentrated within the infected skin remain unknown, we show in mice that the osmotic stress within the $Na^+$-loaded interstitial fluid matrix boosts the antimicrobial host defense and thereby strengthens the anti-infectious barrier function of the skin. The increased cutaneous $Na^+$ concentrations in HSD mice improved *L. major* killing in the $Na^+$ reservoir. We conclude that dietary salt bears a therapeutic potential to promote anti-microbial barrier function of the skin.

The cure of cutaneous leishmaniasis relies on the ability of MΦ to induce *Nos2* and produce high NO levels (Mougneau et al., 2011). Our data suggest that the p38/NFAT5-dependent boost in NOS2-expression in MΦ exposed HS microenvironment *in vitro* and *in vivo* contributes to the enhanced leishmanicidal activity. In addition, salt may activate other

antimicrobial effectors and pathways. Phagosomal acidification and oxidative burst are interconnected with ion fluxes (Soldati and Neyrolles, 2012) and could be sensitive to changes in interstitial $Na^+$ concentration. Furthermore, salt-induced enhancement of inflammatory leukocyte function is not only confined to MΦ, but also evident in T cells (Woehrle et al., 2010). Our finding of increased *Leishmania*-specific T cell responses in HSD mice indicates an additional role of T cells in the salt-driven boost in host defense. We mechanistically focused on MΦ and the role of p38/NFAT5-driven *Nos2*-dependent NO production in the salt-driven boost of host defense. Further investigation of other cells and mechanisms involved in this microenvironment-triggered immune response is warranted in the future.

## Experimental procedures

### Tissue electrolyte analysis, $^{23}$Na MRI and $^{23}$Na spectroscopy of human skin

Chemical analysis of the carcasses included $Na^+$, $K^+$ and water measurements after dry ashing of the skin (Machnik et al., 2009). $^{23}$Na MRI was done as described earlier (Kopp et al., 2012). For $^{23}$Na spectroscopy a $^{23}$Na surface coil was implemented at a 3.0T MR-scanner. Further detailed information and validation of sodium spectroscopy are in supplemental experimental procedures.

### MΦ, RNA interference, immunoblotting, qPCR, and MΦ activation and infection studies

WT and *Nfat5*-overexpressing RAW 246.7 MΦ were used (Machnik et al., 2009). BMM were generated from C57BL/6, *Nos2*$^{-/-}$, *Stat1*$^{-/-}$, Tamoxifen-treated *Cre*-ERT2(T)$^{Cre}$ *Nfat5*$^{fl/fl}$ and *Cre*-ERT2(T)$^{WT/WT}$ *Nfat5*$^{fl/fl}$ or Poly(I:C)-treated Mx$^{WT}$ p38α$^{fl/fl}$ and Mx$^{Cre}$ p38α$^{fl/fl}$ mice. RNA interference, immunoblotting and qPCR was performed as described previously (Machnik et al., 2009). Nitrite and TNF levels were assessed by Griess reaction and ELISA. BMM were infected with *L. major* promastigotes. The extracellular *L. major* were washed off and the BMM were further cultured in the presence of the indicated stimuli for 72 h. The percentage of infected BMM was determined microscopically. For *E. coli* infection, RAW 264.7 cells were infected with *E. coli* and intracellular bacterial load was assessed with a gentamicin protection assay. Further detailed information is in supplemental experimental procedures.

### *In vivo L. major* infection

After two weeks on LSD (<0.1% NaCl, tap water) or HSD diet (4% NaCl, 0.9% saline in the drinking water), we infected hind footpads of FVB mice and/ or LysM$^{WT}$ *Nfat5*$^{fl/fl}$ (control) and LysM$^{Cre}$ *Nfat5*$^{fl/fl}$ mice (FVB background) with $3\times10^6$ of stationary-phase *L. major* promastigotes and continued the respective diet throughout the experiment. The number of parasites in the tissue was determined by limiting dilution analysis (Mahnke et al., 2014). Skin *Nfat5* mRNA levels and skin infiltration of $CD68^+$ MΦ was assessed as described earlier (Machnik et al., 2009). *Leishmania*-specific T cell responses were assessed by *in vitro* restimulation of single-cell suspensions from draining lymph nodes with soluble *Leishmania* antigens (Mahnke et al., 2014). NOS2 expression was analyzed by flow cytometry in $CD11b^+$ lesional cells. Further detailed information is in supplemental experimental procedures.

### Statistical analysis

Results are expressed as means + SEM (if not indicated otherwise). Univariate analysis using the general linear measurement procedure was used to compare data with more than one effector. Other differences were calculated by 1-way ANOVA and appropriate post-hoc tests or Student's *t* test. For non-normally distributed data, the non-parametric Mann-Whitney-test was used. *P*-values of <0.05 (*) were deemed statistically significant (if not indicated otherwise). SPPS Statistics (version 21.0, IBM) or Prism v4.0 and v6.0 (GraphPad software) were used.

## Supplementary Material

Refer to Web version on PubMed Central for supplementary material.

## Acknowledgments

The Deutsche Forschungsgemeinschaft (DFG; SFB 643 A6 & B16; DA1067/7-2) supported J.J., J.P.D, C.B. and J.T. J.T. was also supported by the German Ministry for Economics and Technology (50WB1218), the Interdisciplinary Center for Clinical Research (IZKF) Erlangen, and the NIH (RO1 HL118579-01), C.B. by the IZKF Erlangen (A61) and the Emerging Field Initiative of the FAU. K.J.B. received an Australian National Health and Medical Research Council C. J. Martin Fellowship (APP1037633). The DFG and the German Center for Cardiovascular Research supported D.N.M. and F.C.L. We thank the Imaging Science Institute (Erlangen) for measurement time and for technical support. We are grateful for the excellent technical assistance of Kirstin Castiglione, Andrea Debus, Heidi Sebald, Jenny Hähnel, Sabrina Cabric, Anna Birukov, Monika Nowottny and Daniela Amslinger.

## References

Angrisano T, Lembo F, Peluso S, Keller S, Chiariotti L, Pero R. Helicobacter pylori regulates iNOS promoter by histone modifications in human gastric epithelial cells. Med Microbiol Immunol. 2012; 201:249–257. [PubMed: 22215089]

Belkaid Y, Segre JA. Dialogue between skin microbiota and immunity. Science. 2014; 346:954–959. [PubMed: 25414304]

Braff MH, Gallo RL. Antimicrobial peptides: an essential component of the skin defensive barrier. Current topics in microbiology and immunology. 2006; 306:91–110. [PubMed: 16909919]

Buxade M, Lunazzi G, Minguillon J, Iborra S, Berga-Bolanos R, Del Val M, Aramburu J, Lopez-Rodriguez C. Gene expression induced by Toll-like receptors in macrophages requires the transcription factor NFAT5. J Exp Med. 2012; 209:379–393. [PubMed: 22312110]

Denkert C, Warskulat U, Hensel F, Haussinger D. Osmolyte strategy in human monocytes and macrophages: involvement of p38MAPK in hyperosmotic induction of betaine and myoinositol transporters. Arch Biochem Biophys. 1998; 354:172–180. [PubMed: 9633613]

Diefenbach A, Schindler H, Donhauser N, Lorenz E, Laskay T, MacMicking J, Rollinghoff M, Gresser I, Bogdan C. Type 1 interferon (IFNalpha/beta) and type 2 nitric oxide synthase regulate the innate immune response to a protozoan parasite. Immunity. 1998; 8:77–87. [PubMed: 9462513]

Fischer CL, Blanchette DR, Brogden KA, Dawson DV, Drake DR, Hill JR, Wertz PW. The roles of cutaneous lipids in host defense. Biochim Biophys Acta. 2014; 1841:319–322. [PubMed: 23994607]

Furuse M, Hata M, Furuse K, Yoshida Y, Haratake A, Sugitani Y, Noda T, Kubo A, Tsukita S. Claudin-based tight junctions are crucial for the mammalian epidermal barrier: a lesson from claudin-1-deficient mice. The Journal of cell biology. 2002; 156:1099–1111. [PubMed: 11889141]

Gaddy JA, Radin JN, Loh JT, Zhang F, Washington MK, Peek RM Jr, Algood HM, Cover TL. High dietary salt intake exacerbates Helicobacter pylori-induced gastric carcinogenesis. Infect Immun. 2013; 81:2258–2267. [PubMed: 23569116]

Go WY, Liu X, Roti MA, Liu F, Ho SN. NFAT5/TonEBP mutant mice define osmotic stress as a critical feature of the lymphoid microenvironment. Proc Natl Acad Sci U S A. 2004; 101:10673–10678. [PubMed: 15247420]

Han J, Lee JD, Bibbs L, Ulevitch RJ. A MAP kinase targeted by endotoxin and hyperosmolarity in mammalian cells. Science. 1994; 265:808–811. [PubMed: 7914033]

Hofmeister LH, Perisic S, Titze J. Tissue sodium storage for kidney-like extrarenal countercurrent systems? Pflugers Arch. 2015 in press.

Ivanova LN, Archibasova VK, Shterental I. Sodium-depositing function of the skin in white rats. Fiziol Zh SSSR Im I M Sechenova. 1978; 64:358–363. [PubMed: 648666]

Junger WG, Liu FC, Loomis WB, Hoyt DB. Hypertonic saline solution as disinfectant. East Afr Med J. 1994; 71:83. [PubMed: 7925049]

Kawai T, Akira S. The role of pattern-recognition receptors in innate immunity: update on Toll-like receptors. Nature immunology. 2010; 11:373–384. [PubMed: 20404851]

Kleinewietfeld M, Manzel A, Titze J, Kvakan H, Yosef N, Linker RA, Muller DN, Hafler DA. Sodium chloride drives autoimmune disease by the induction of pathogenic TH17 cells. Nature. 2013; 496:518–522. [PubMed: 23467095]

Ko BC, Lam AK, Kapus A, Fan L, Chung SK, Chung SS. Fyn and p38 signaling are both required for maximal hypertonic activation of the osmotic response element-binding protein/tonicity-responsive enhancer-binding protein (OREBP/TonEBP). J Biol Chem. 2002; 277:46085–46092. [PubMed: 12359721]

Ko BC, Turck CW, Lee KW, Yang Y, Chung SS. Purification, identification, and characterization of an osmotic response element binding protein. Biochem Biophys Res Commun. 2000; 270:52–61. [PubMed: 10733904]

Kopp C, Linz P, Dahlmann A, Hammon M, Jantsch J, Muller DN, Schmieder RE, Cavallaro A, Eckardt KU, Uder M, Luft FC, Titze J. 23Na magnetic resonance imaging-determined tissue sodium in healthy subjects and hypertensive patients. Hypertension. 2013; 61:635–640. [PubMed: 23339169]

Kopp C, Linz P, Wachsmuth L, Dahlmann A, Horbach T, Schofl C, Renz W, Santoro D, Niendorf T, Muller DN, Neininger M, Cavallaro A, Eckardt KU, Schmieder RE, Luft FC, Uder M, Titze J. (23)Na magnetic resonance imaging of tissue sodium. Hypertension. 2012; 59:167–172. [PubMed: 22146510]

Lang KS, Fillon S, Schneider D, Rammensee HG, Lang F. Stimulation of TNF alpha expression by hyperosmotic stress. Pflugers Arch. 2002; 443:798–803. [PubMed: 11889578]

Lee KM, Danuser R, Stein JV, Graham D, Nibbs RJ, Graham GJ. The chemokine receptors ACKR2 and CCR2 reciprocally regulate lymphatic vessel density. Embo J. 2014; 33:2564–2580. [PubMed: 25271254]

Liew FY, Millott S, Parkinson C, Palmer RM, Moncada S. Macrophage killing of Leishmania parasite in vivo is mediated by nitric oxide from L-arginine. J Immunol. 1990; 144:4794–4797. [PubMed: 2351828]

Linz P, Santoro D, Renz W, Rieger J, Ruehle A, Ruff J, Deimling M, Rakova N, Muller DN, Luft FC, Titze J, Niendorf T. Skin sodium measured with (23) Na MRI at 7.0 T. NMR in biomedicine. 2015; 28:54–62. [PubMed: 25328128]

Lopez-Rodriguez C, Aramburu J, Rakeman AS, Rao A. NFAT5, a constitutively nuclear NFAT protein that does not cooperate with Fos and Jun. Proc Natl Acad Sci U S A. 1999; 96:7214–7219. [PubMed: 10377394]

Machnik A, Neuhofer W, Jantsch J, Dahlmann A, Tammela T, Machura K, Park JK, Beck FX, Muller DN, Derer W, Goss J, Ziomber A, Dietsch P, Wagner H, van Rooijen N, Kurtz A, Hilgers KF, Alitalo K, Eckardt KU, Luft FC, Kerjaschki D, Titze J. Macrophages regulate salt-dependent volume and blood pressure by a vascular endothelial growth factor-C-dependent buffering mechanism. Nat Med. 2009; 15:545–552. [PubMed: 19412173]

Mahnke A, Meier RJ, Schatz V, Hofmann J, Castiglione K, Schleicher U, Wolfbeis OS, Bogdan C, Jantsch J. Hypoxia in Leishmania major skin lesions impairs the NO-dependent leishmanicidal activity of macrophages. J Invest Dermatol. 2014; 134:2339–2346. [PubMed: 24583949]

Miyakawa H, Woo SK, Dahl SC, Handler JS, Kwon HM. Tonicity-responsive enhancer binding protein, a Rel-like protein that stimulates transcription in response to hypertonicity. P Natl Acad Sci USA. 1999; 96:2538–2542.

Mougneau E, Bihl F, Glaichenhaus N. Cell biology and immunology of Leishmania. Immunol Rev. 2011; 240:286–296. [PubMed: 21349100]

Murray PJ, Wynn TA. Protective and pathogenic functions of macrophage subsets. Nat Rev Immunol. 2011; 11:723–737. [PubMed: 21997792]

Padtberg. Über die Bedeutung der Haut als Chlordepot. Arch exp Path Pharm. 1909:60–79.

Paling D, Solanky BS, Riemer F, Tozer DJ, Wheeler-Kingshott CAM, Kapoor R, Golay X, Miller DH. Sodium accumulation is associated with disability and a progressive course in multiple sclerosis. Brain. 2013; 136:2305–2317. [PubMed: 23801742]

Proksch E, Brandner JM, Jensen JM. The skin: an indispensable barrier. Exp Dermatol. 2008; 17:1063–1072. [PubMed: 19043850]

Rauch I, Muller M, Decker T. The regulation of inflammation by interferons and their STATs. Jak-Stat. 2013; 2:e23820. [PubMed: 24058799]

Roth I, Leroy V, Kwon HM, Martin PY, Feraille E, Hasler U. Osmoprotective transcription factor NFAT5/TonEBP modulates nuclear factor-kappaB activity. Mol Biol Cell. 2010; 21:3459–3474. [PubMed: 20685965]

Schroder JM. The role of keratinocytes in defense against infection. Current opinion in infectious diseases. 2010; 23:106–110. [PubMed: 20010101]

Schwartz L, Guais A, Pooya M, Abolhassani M. Is inflammation a consequence of extracellular hyperosmolarity? J Inflamm (Lond). 2009; 6:21. [PubMed: 19549308]

Shapiro L, Dinarello CA. Osmotic regulation of cytokine synthesis in vitro. Proc Natl Acad Sci U S A. 1995; 92:12230–12234. [PubMed: 8618875]

Shapiro L, Dinarello CA. Hyperosmotic stress as a stimulant for proinflammatory cytokine production. Exp Cell Res. 1997; 231:354–362. [PubMed: 9087177]

Soldati T, Neyrolles O. Mycobacteria and the intraphagosomal environment: take it with a pinch of salt(s)! Traffic. 2012; 13:1042–1052. [PubMed: 22462580]

Titze J, Shakibaei M, Schafflhuber M, Schulze-Tanzil G, Porst M, Schwind KH, Dietsch P, Hilgers KF. Glycosaminoglycan polymerization may enable osmotically inactive Na+ storage in the skin. Am J Physiol Heart Circ Physiol. 2004; 287:H203–208. [PubMed: 14975935]

Tunggal JA, Helfrich I, Schmitz A, Schwarz H, Gunzel D, Fromm M, Kemler R, Krieg T, Niessen CM. E-cadherin is essential for in vivo epidermal barrier function by regulating tight junctions. Embo J. 2005; 24:1146–1156. [PubMed: 15775979]

Wahlgren V. Über die Bedeutung der Gewebe als Chlordepots. Arch exp Path Pharm. 1909; 61:97–112.

Warner RR, Myers MC, Taylor DA. Electron probe analysis of human skin: determination of the water concentration profile. J Invest Dermatol. 1988; 90:218–224. [PubMed: 3339263]

Wiig H, Schroder A, Neuhofer W, Jantsch J, Kopp C, Karlsen TV, Boschmann M, Goss J, Bry M, Rakova N, Dahlmann A, Brenner S, Tenstad O, Nurmi H, Mervaala E, Wagner H, Beck FX, Muller DN, Kerjaschki D, Luft FC, Harrison DG, Alitalo K, Titze J. Immune cells control skin lymphatic electrolyte homeostasis and blood pressure. J Clin Invest. 2013; 123:2803–2815. [PubMed: 23722907]

Woehrle T, Yip L, Manohar M, Sumi Y, Yao Y, Chen Y, Junger WG. Hypertonic stress regulates T cell function via pannexin-1 hemichannels and P2X receptors. J Leukoc Biol. 2010; 88:1181–1189. [PubMed: 20884646]

Wu C, Yosef N, Thalhamer T, Zhu C, Xiao S, Kishi Y, Regev A, Kuchroo VK. Induction of pathogenic TH17 cells by inducible salt-sensing kinase SGK1. Nature. 2013; 496:513–517. [PubMed: 23467085]

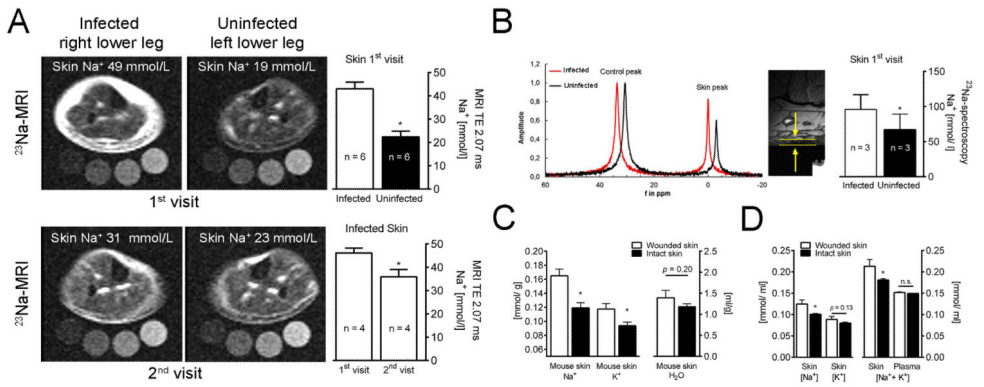


**Fig. 1. Infection increases $Na^+$ storage in skin of man and mouse**

**(A)** $^{23}Na$ MRI of an infected and contralateral uninfected lower leg with bacterial skin infection. Upper left panel, acute ($1^{st}$) visit; lower left panel, 28 days after antibiotics ($2^{nd}$ visit). Upper right panel, $^{23}Na$ MRI estimates of $1^{st}$ visit (mmol/l relative to standards; mean + SEM; n = 6). Lower right panel, $^{23}Na$ MRI estimates (mmol/ l relative to standards) of $1^{st}$ & $2^{nd}$ visit (mean + SEM; n = 4). TE: echo time in ms. **(B)** Skin $^{23}Na$ magnetic resonance spectrogram at $1^{st}$ visit (skin peak). Control peak (100 mmol/l $Na^+$ standard with shift reagent). High resolution $^1H$ image for determination of skin thickness (arrows and bars). Skin $Na^+$ concentrations (mean + SEM; n = 3). **(C & D)** $Na^+$, $K^+$ and water distribution in plasma and skin of animals with wounded skin (mean + SEM; n ≥ 6/group; <0.1% NaCl chow, tap water). Skin water, $Na^+$, and $K^+$ contents were measured. **(C)** $Na^+$, $K^+$ and $H_2O$ content per g dry weight. **(D)** $Na^+$-to-water, $K^+$-to-water and ($Na^+$+$K^+$)-to-water ratios.

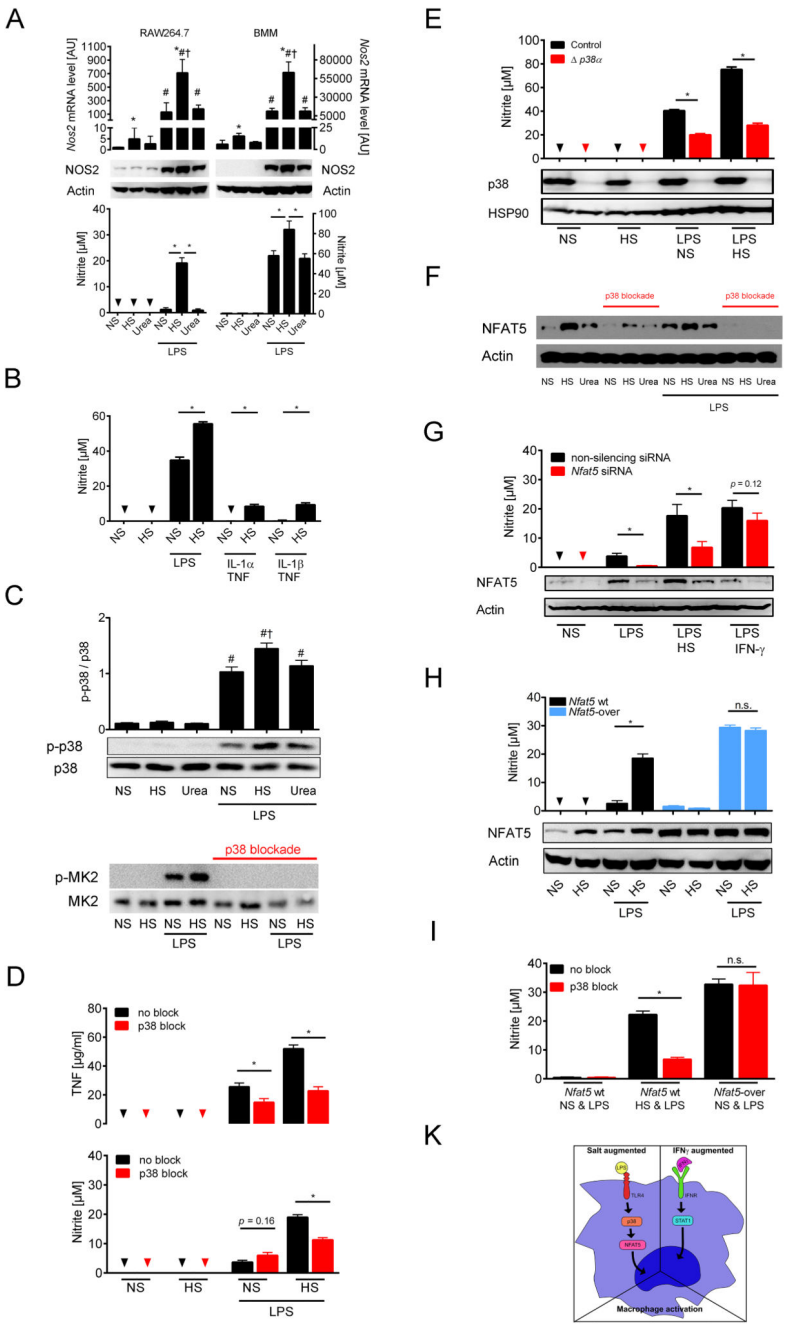


**Fig. 2. High salt augmented LPS-induced MΦ activation requires p38/MAPK-dependent NFAT5-signalling**

**(A)** RAW 264.7 MΦ (left panel) and bone marrow-derived MΦ (BMM, right panel) were cultured in normal cell culture medium (NS: normal salt), with additional 40 mM NaCl in the medium (HS: high salt) or 80 mM urea ± 10 ng/ ml LPS for 24 h. *Nos2* mRNA (mean + SEM; n = 4 (RAW264.7); n = 4–5 (BMM)), * *P*(HS) < 0.05; # *P*(LPS) < 0.05; † *P*(LPS*HS) < 0.05; NOS2 protein, and nitrite levels (mean + SEM; n = 4 (RAW264.7); n = 11 (BMM)); Triangles: not detectable (n.d.). **(B)** BMM were cultured in NS, with HS ± LPS (1 ng/ ml), IL-1α (50 ng/ ml) or IL-1β (50 ng/ ml) + TNF (20 ng/ ml) for 24 h. Nitrite levels (mean +

SEM; 4 similar experiments); Triangles: n.d. *$P < 0.05$ **(C)** RAW 264.7 MΦ were cultured in NS, with HS or 80 mM urea ± LPS (10 ng/ ml) for 45 min. Upper panel, densitometry and immunoblotting of p38/MAPK and activated p-p38/MAPK (mean + SEM; n=8). # $P$(LPS) < 0.05; † $P$(LPS*HS) < 0.05. Lower panel, immunoblotting detected the p38/MAPK substrate MK2 and activated p-MK2. **(D)** RAW 264.7 MΦ were pretreated ± p38 blocker SB203580. After ½ h cells were cultured in NS, with HS ± 10 ng/ ml LPS for 24 h. Upper panel, TNF levels (mean + SEM; n = 2 in triplicates); lower panel, nitrite levels (n=7). Triangles: n.d. **(E)** BMM from Poly(I:C)-treated $Mx^{WT}$ $p38\alpha^{fl/fl}$ (control) and $Mx^{Cre}$ $p38\alpha^{fl/fl}$ (Δ *p38*α) mice were cultured in NS, with HS ± LPS (1 ng/ ml) for 24 h. Upper panel, nitrite levels (mean + SEM; n = 2 in quadruplicates); Triangles: n.d.; Lower panel, immunoblotting of p38/MAPK and HSP90. **(F)** As (D). Immunoblotting of NFAT5 and Actin. **(G)** RAW 264.7 MΦ electroporated with control non-silencing siRNA or *Nfat5*-specific siRNA (*Nfat5* siRNA) were cultured in NS or HS ± LPS (10 ng/ ml) or LPS/ IFN-γ under NS for 24 h. Immunoblotting of NFAT5 and Actin. Nitrite levels (mean + SEM; n = 3–4). **(H)** RAW 264.7 wild-type MΦ (*Nfat5* wt) and RAW 264.7 MΦ with stable *Nfat5* overexpression (*Nfat5*-over) were cultured NS or HS ± LPS (10 ng/ ml) for 24 h. Immunoblotting of NFAT5 and Actin. Nitrite levels (mean + SEM; n = 4). **(I)** As (D) but in addition RAW 264.7 MΦ with stable *Nfat5* overexpression (*Nfat5*-over) were used. A representative experiment in quintuplicates out of two independent experiments is displayed. **(K)** Schematic of HS-induced alterations in MΦ LPS-signaling.

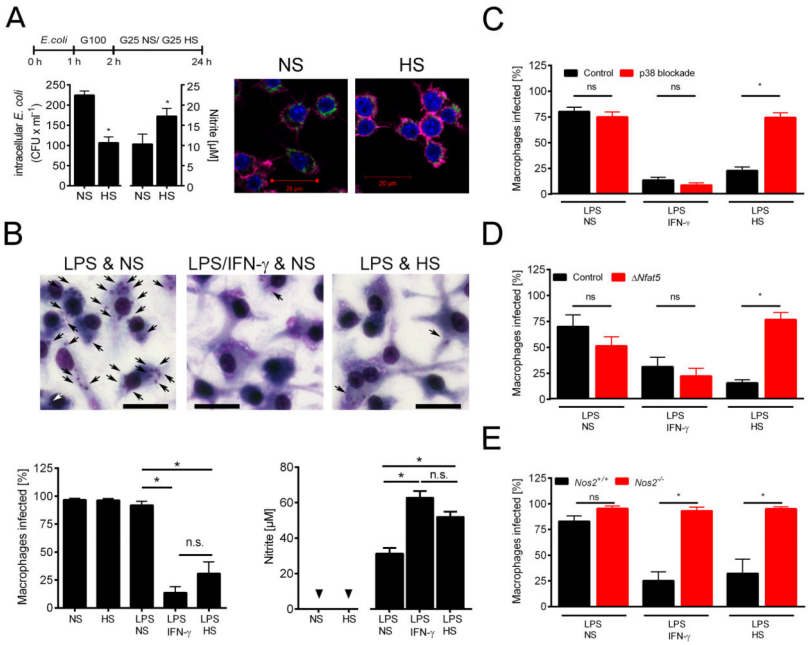


**Fig. 3. High salt conditions promote anti-microbial activity via p38/MAPK-dependent NFAT5 signaling**

**(A)** RAW 264.7 MΦ were infected with *E. coli* incubated under NS and HS conditions. Left panel, after 24 h intracellular bacterial load and nitrite levels (mean + SEM; n = 2 at least in triplicates). Right panel, after 24 h cells were fixed. GFP-*E. coli*, green. Phalloidin (Actin), purple. DAPI (DNA), blue. Scale bar = 20 µm. **(B)** BMM were infected with *L. major* promastigotes and stimulated with LPS (20 ng/ ml) in NS or HS medium or with IFN-γ (20 ng/ ml) under NS. Upper panel, Diff-Quik stains of BMM after 72 h. Intracellular parasites, black arrows. Scale bar = 20 µm. Lower panels, percent of infected BMM (mean + SEM; n = 5) and nitrite levels (mean + SEM; n = 7). **(C)** *L. major*-infected BMM were treated with SB203580 and stimulated as described in (A). Percent of infected BMM (mean + SEM; n = 5). **(D)** As (B) but BMM from Tamoxifen-treated *Cre*-ERT2(T)$^{Cre}$ *Nfat5*$^{fl/fl}$ (Δ*Nfat5*) and *Cre*-ERT2(T)$^{WT/WT}$ *Nfat5*$^{fl/fl}$ (control) mice were used (mean + SEM; n = 3). **(E)** As (B) but *Nos2*$^{+/+}$ and *Nos2*$^{-/-}$ BMM were used (mean + SEM; n=3–4). Triangles: n.d.

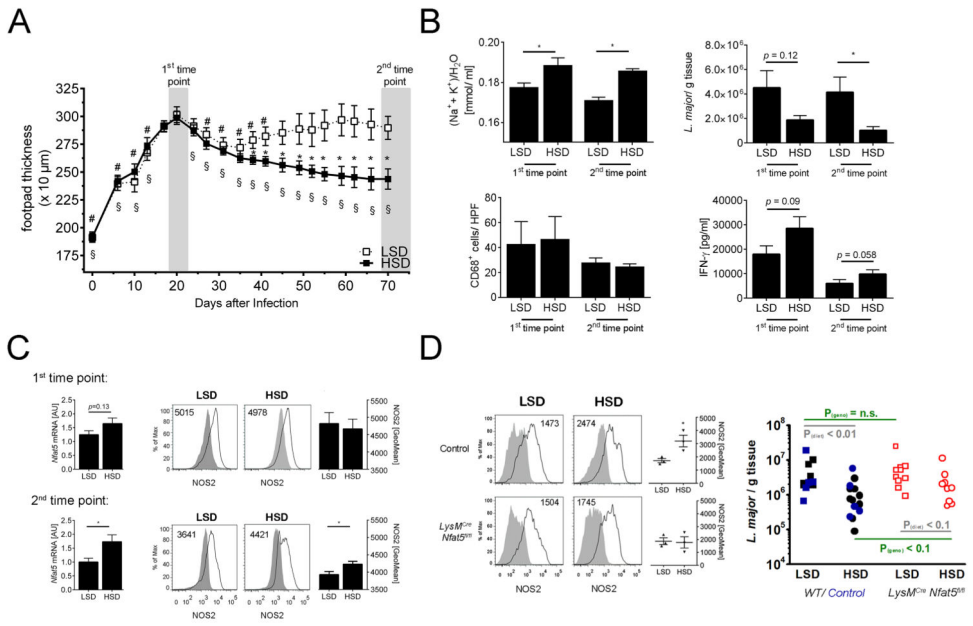


**Fig. 4. High salt diet ameliorates *L. major* infection *in vivo***

**(A–C)** FVB WT mice were fed low salt (LSD) or high salt-diet (HSD) throughout the experiment and infected with *L. major* promastigotes in their footpads two weeks after initiation of the respective diet. The diets were continued throughout the experiment. **(A)** Lesion development of LSD and HSD mice (means ± 95% CI; n = 8/ group). * *P*(vs. LSD) < 0.01; # *P*(vs. day 20 LSD) < 0.01; § *P*(vs. day 20 HSD) < 0.01 **(B)** At the 1st time point (20–24 days after infection) and at the 2nd time point (at the end of experiment) $Na^+$, $K^+$ and water distribution (mean + SEM; n ≥ 6/ group), parasite burden (mean + SEM; n ≥ 7/ group), amount of lesional $CD68^+$ MΦ (mean + SEM; n ≥ 3/ group) and *Leishmania*-specific T cell responses (mean + SEM; n ≥ 4/ group) are given. **(C)** Skin *Nfat5* mRNA levels (left panel; mean + SEM; n ≥ 4) and geometric mean fluorescence of NOS2-protein expression in lesional $CD11b^+$ cells (right panel; mean + SEM; n=4–5/ group) at the 1st time point and at the 2nd time point. Representative histograms of NOS2-expression in lesional $CD11b^+$ cells are displayed. Insets: geometric mean fluorescence of NOS2. Grey filled area: isotype control. Black solid line: NOS2-expression. **(D)** $LysM^{WT}$ $Nfat5^{fl/fl}$ (control) and $LysM^{Cre}$ $Nfat5^{fl/fl}$ were fed LSD and HSD and infected with *L. major* as described above. Left panel, as in (C) at the end of the experiment NOS2-protein expression in lesional $CD11b^+$ cells is given (mean + SEM; n=3/ group). Right panel, WT mice (black colored), $LysM^{Cre}$ $Nfat5^{fl/fl}$ (red colored) and $LysM^{WT}$ $Nfat5^{fl/fl}$ (controls, blue colored) were fed low salt (LSD) or high salt-diet (HSD) and infected with *L. major* promastigotes in their footpads. Parasite burden (n=9–14/ group) in skin lesions of infected mice on a HSD or LSD for over 70 days.